

# Improvements on the Diagnostic Residual Gas Analyzer at Wendelstein 7-X

Georg Schlisio<sup>1</sup>, Fabio A. Ravelli<sup>1</sup>, C. Christopher Klepper<sup>1</sup>, *Senior Member, IEEE*, Jeffrey H. Harris<sup>1</sup>, Theodore M. Biewer<sup>1</sup>, Chris Marcus<sup>1</sup>, Amit K. Kharwandikar<sup>1</sup>, Dirk Naujoks<sup>1</sup>, and Thierry Kremeyer<sup>1</sup>

**Abstract**—Exhaust gas analysis provides key information on fusion processes, divertor operation, and wall state in fusion experiments and future reactors. The diagnostic residual gas analyzer (DRGA) concept has been developed for ITER with a focus on fast helium and hydrogen isotope detection. The first operation of the prototype DRGA (P-DRGA) at the stellarator Wendelstein 7-X showed potential for improvement in terms of magnetic sensor shielding, data acquisition automation, and potential new additions to the cluster of sensors on the P-DRGA. More recently, a Monte Carlo simulation of the flow of the mixed gas species effluent from the pressure-reducing orifice, down to about 8-m sampling tube and into the analysis region of the sensors, has been found to generally agree with previous calculations and measurements but revealed potential back-streaming effects for light gases, with impact on detection limits both for the prototype and for the ITER DRGA currently in design. For the upcoming campaign of the prototype, an enhanced soft iron shield will safeguard the gauges against magnetic stray field influence. The newly introduced shielding has been tested for its effect on magnetic stray fields and found to reduce the inside residual field by about two orders of magnitude.

**Index Terms**—Electromagnetic shielding, fusion reactor design, vacuum technology.

## I. INTRODUCTION

THE diagnostic residual gas analyzer (DRGA) was developed to aid in detecting and monitoring sub divertor gas composition for both fusion exhaust control and general vacuum monitoring [1].

The prototype DRGA (P-DRGA) [2] developed for ITER was deployed to Wendelstein 7-X (W7-X) to gain experience with the system in operation outside the laboratory. The optimized modular stellarator experiment W7-X [3] offers unique testing capabilities for diagnostics due to its steady-state capabilities.

Manuscript received January 28, 2022; revised April 30, 2022; accepted June 1, 2022. The review of this article was arranged by Senior Editor G. H. Neilson. (*Corresponding author: Georg Schlisio.*)

Georg Schlisio, Amit K. Kharwandikar, Dirk Naujoks, and Thierry Kremeyer are with the Max Planck Institute for Plasma Physics, 17491 Greifswald, Germany (e-mail: georg.schlisis@ipp.mpg.de).

Fabio A. Ravelli was with the Oak Ridge National Laboratory, Oak Ridge, TN 37831 USA. He is now with Commonwealth Fusion Systems, Cambridge, MA 02139 USA.

C. Christopher Klepper, Jeffrey H. Harris, Theodore M. Biewer, and Chris Marcus are with the Oak Ridge National Laboratory, Oak Ridge, TN 37831 USA.

Color versions of one or more figures in this article are available at <https://doi.org/10.1109/TPS.2022.3183580>.

Digital Object Identifier 10.1109/TPS.2022.3183580

We present here the progress of technical enhancements in view of the next experimental campaign of the P-DRGA at W7-X, namely, enhanced magnetic shielding and better understanding of gas flow in the system.

Section II gives a short overview over the divertor changes of W7-X, Section III introduces the new magnetic shielding and its testing, and Section IV shows the results of the gas flow simulations. Prospects for the evolution of the optical gas analyzer (OGA) are discussed in Section V, and an overview of further smaller changes and a summary conclude this article.

## II. W7-X SUBDIVERTOR CHANGES

The P-DRGA, outfitted with a sampling tube, operated for first integral tests of the DRGA system [4] in the W7-X initial divertor experiment campaign, OP1.2. In the upcoming experiment campaign, OP2, W7-X will operate a new fully water cooled first wall from carbon fiber composite, the so-called high-heat-flux (HHF) divertor, allowing for higher plasma performance and thus higher sub divertor pressure. A more restricted sub divertor space and an improved divertor closure also aide that goal. The additional introduction of cryo vacuum pump (CVP) in the sub divertor space is expected to reduce gas flux at the P-DRGA sampling tube tip during CVP operation. Fig. 1 shows a comparison of old and new sub divertor cross sections in similar positions. Due to difficulties in predicting the future working point and effect of the aforementioned changes on the sub divertor pressure, the previous orifice design was left untouched, and the first observations about the changes will be made in OP2.1 before adaptations to the orifice size are considered.

## III. MAGNETIC SHIELDING

The previously installed gauge shielding, consisting of a two-layer strapped-on permalloy foil wound cylindrically around the device, was found to be insufficient, and the P-DRGA suffered from magnetic interference during its campaign in 2018 as reported in [4]. The maximum ambient magnetic field of up to 5 mT leads to saturation of the foil and subsequent disturbance of the measurement process, which is based on free streaming charged particles in carefully controlled electric fields.

To counteract this disturbance, the previous shielding has been replaced by a soft iron cylinder with a wall thickness

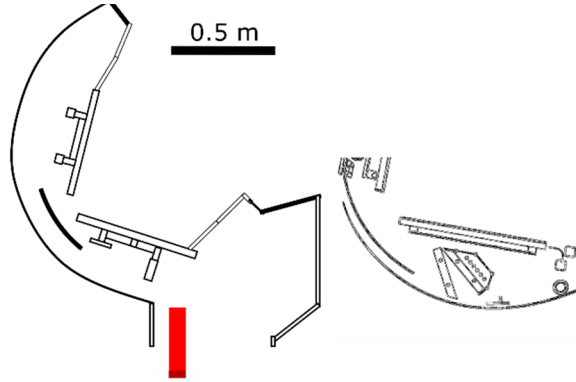


Fig. 1. Illustration of the subdivertor geometry shown by a toroidal cut through the pumping gap at the low-iota divertor target. Left: Situation as of OP1.2, with the test divertor unit and no CVP installed. The pumping port is shown as vessel opening at the bottom right-hand side, with the DRGA position in red. Right: Situation at a similar position in OP2, with the HHF divertor and CVP. While the position of the cuts in both images does not exactly match, the far more constricted volume with the CVP is clearly visible. Its negative influence on conductance between pumping gap and pumping port is obvious.

of 1 cm. The shielding efficiency was further improved with an inner lining of permalloy foil. Since multilayer shielding is most efficient with air gaps [5], a gap was introduced between the soft iron and the permalloy layer. For mechanical stability, the gap was made with two layers of 0.25-mm-thick aluminum sheet, which has a relative magnetic permeability very close to air. The resulting layer structure is flexible enough to allow easy installation at the gauge flange, while still maximizing the gap width and thus the shielding efficiency. Air-gapped magnetic shielding is known to greatly enhance shielding efficiency. An illustration and further discussion are given in Fig. 12.1 panel c of [5].

To quantify shielding efficiency, measurements were conducted at the VINETA facility [6]. The shielding was subjected to about 5 mT both parallel and perpendicular to the cylinder axis, and the residual field inside the shielding was measured with a magnetometer probe in both magnetic field orientations along the cylinder axis. The measurement was conducted thrice, once without shielding as baseline to confirm that the chamber models the conditions expected in the torus hall sufficiently well, once with the plain soft iron cylinder (“shielding”), and once with the additional permalloy lining (“lined shielding”). The results of the measurement along with the derived attenuation factor are shown in Fig. 2.

The magnetic field in the VINETA chamber was found to be sufficiently homogeneous both along the axis (low ripple) and across the chamber, dropping down to 4.3 mT at the farthest point outward.

While the permalloy lining does not change the shielding efficiency much for magnetic fields parallel to the shielding axis, it reduces drastically the magnetic field strength in a broad region around the center of the cylinder for perpendicular magnetic field. This is about where the analyzer will be situated, which suggests much smaller interference with the measurement using the new shielding. During operation, the magnetic field vector at the shielding is expected to vary greatly between W7-X magnetic field configurations due

to the quadrupole falloff effect. Given the mass spectrometers’ manufacturers claim of magnetic field acceptance up to 0.5 mT, the shown shielding effect is expected to efficiently shield both parallel and perpendicular components and ensure an unperturbed operation of the mass spectrometers in the upcoming campaigns.

#### IV. MONTE CARLO FLOW ANALYSIS

Molflow+ is a *Test Particle Monte Carlo Method* code largely used to study the pressure profiles of particle accelerators. In many cases, these vacuum systems present lumped vacuum pumps connected by long beamlines; in such cases, a Monte Carlo approach gives more accurate results respect to analytical calculations that cannot take into consideration the pressure anisotropies generated by an elongated vacuum structure. It allows the calculation of a multitude of parameters, such as pressure profiles, effective pumping speeds, adsorption distributions, in-vessel residence times (IVRTs), and more [7], [8]. As the name suggests, it is restricted to the molecular flow regime.

Here, it is used to confirm analytical calculations from the design phase of the sampling tube [4] as well as measurements from the initial measurement campaign, especially the gas propagation time through the system [time of flight (TOF)] as well as yielded pressures at the measurement position. A similar analysis has been performed for the ITER DRGA in [9].

For calculation, the code requires a 3-D mesh representing the vacuum boundaries, which was obtained from the mechanical CAD drawing of the P-DRGA by reducing the model complexity to a suitable level. Details of the vacuum boundary, the sampling tube tip and the analysis chamber, can be seen in Fig. 3. In first approximation, the model does not include the electron cyclotron heating (ECH) filter in front of the orifice.

The code also requires the input of turbo molecular pump (TMP) pumping speed, which was obtained from a vendor data sheet.

##### A. Throughput and Pressure at RGA

The calculations regarding the dimensions of the sampling orifice are made considering H<sub>2</sub> as the dominant partial pressure on the divertor side. This simplifying assumption results in a conservative value for all the gases in view of the lowest TMP pumping speed and of the highest orifice conductance for this gas. Furthermore, molecular flow regime along the flight tube and 293.15 K is considered. Because the employed orifice is very thin, it is possible to calculate the throughput injected in the DRGA by using a zero-length approximation. In this case, assuming molecular flow conditions and with the outlet pressure being negligible with respect to the inlet pressure  $p_{in}$ , the throughput  $q$  of an orifice of area  $A$  can be expressed in terms of the pressure difference  $\Delta p$ , the mean velocity  $\bar{v}$ , temperature  $T$ , gas constant  $R$ , and molecular mass  $M_{mol}$  as follows:

$$q = \frac{\bar{v}}{4} A \cdot \Delta p \simeq \frac{1}{4} \sqrt{\frac{8RT}{\pi M_{mol}}} A \cdot p_{in}.$$

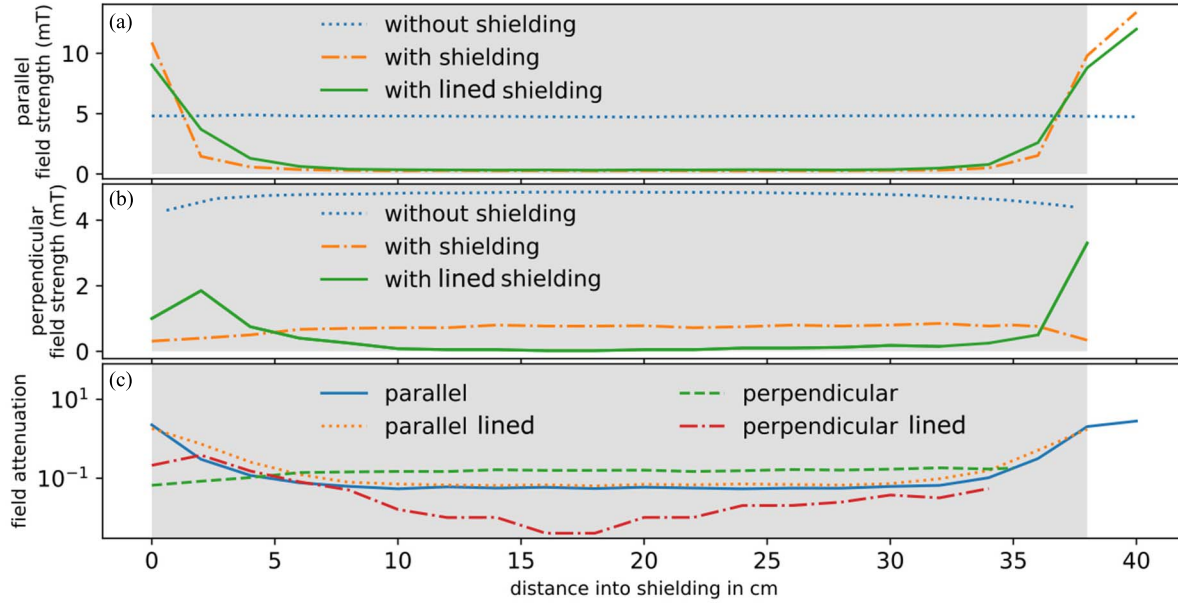


Fig. 2. Measured magnetic field strengths without shielding and with shielding (a) parallel and (b) perpendicular to the shielding cylinder axis. The soft-iron cylinder with additional permalloy lining is denoted as lined shielding. (c) Shielding efficiency, given by the ratio of unshielded and shielded magnetic field. The shaded area indicates the length of the shielding cylinder. The analyzer sits in the shielding center, and the length of the active component is about 10 cm. (Color online.)

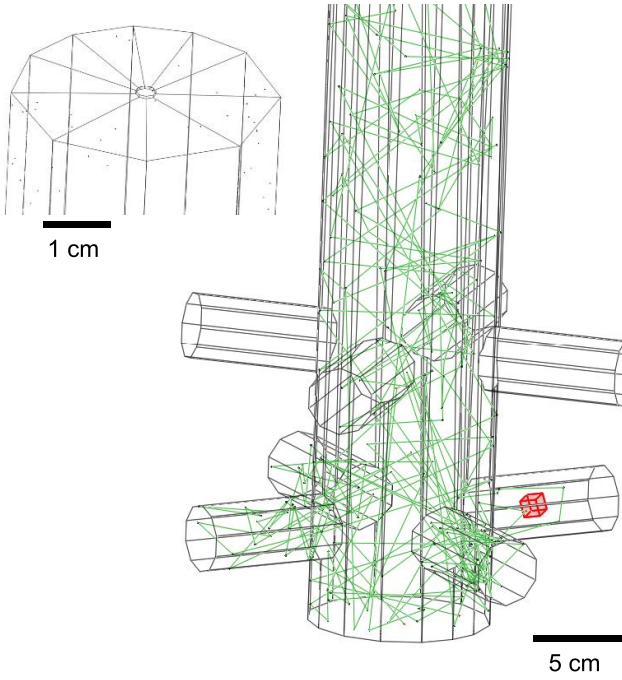


Fig. 3. Vacuum boundary representation of the analysis P-DRGA chamber with instrument ports. Test particle traces in green, and gauge cube in red. The inset in the top left corner shows a rendering of the inlet orifice. (Color online.)

With a 0.1-Pa maximum subdivertor pressure and an orifice area of  $7.07 \times 10^{-6} \text{ m}^2$ , the maximum H<sub>2</sub> throughput is calculated as  $3.1 \times 10^{-4} \text{ Pa} \cdot \text{m}^3/\text{s}$ . A simulation with the calculated maximum H<sub>2</sub> throughput injected at the orifice, see inset in Fig. 3, confirmed a maximum pressure at residual gas analysis (RGA) of  $1.84 \times 10^{-3} \text{ Pa}$  very close to the design pressure of  $10^{-3} \text{ Pa}$ .

TABLE I  
ENUMERATION OF GAUGE CUBE FACES, MEASURED DENSITY, AND DERIVED PRESSURE AND THE CORRESPONDING AVERAGED VOLUME DENSITY AND PRESSURE. THE GAUGE CUBE IS SHOWN IN RED IN Fig. 3

Face	Density (m <sup>-3</sup> )	Pressure (Pa)
Top	$1.06 \cdot 10^{17}$	$8.25 \cdot 10^{-4}$
L1	$1.46 \cdot 10^{17}$	$1.12 \cdot 10^{-3}$
L2	$1.19 \cdot 10^{17}$	$9.79 \cdot 10^{-4}$
L3	$1.18 \cdot 10^{17}$	$9.73 \cdot 10^{-4}$
L4	$1.25 \cdot 10^{17}$	$9.79 \cdot 10^{-4}$
Bottom	$1.19 \cdot 10^{17}$	$9.78 \cdot 10^{-4}$
Average	$1.22 \cdot 10^{17}$	$9.76 \cdot 10^{-4}$
Average corrected	$2.3 \cdot 10^{17}$	$1.86 \cdot 10^{-3}$

To take into account possible anisotropy, the simulated pressure at the RGA was calculated by considering a small gauge cube of 1 cm side length, transparent to the gas particles, and placed into the RGA DN40 pipe, shown in red in Fig. 3. Molflow+ calculates the average density and the average pressure projected on the gauge cube faces; these values are reported in Table I. The density in the cube is given by the average of the six values and it needs to be corrected with a geometrical factor  $6/\pi$  so to switch to a spherical volume. The pressure is then calculated by plugging the average density in the ideal gas law:  $p = (n/V)kT$ .

#### B. In-Vessel Residence Time

Molflow+ traces each test particle and records the time and location of any contact of the particle with the vacuum chamber walls, until the test particle is pumped away leaving

TABLE II

MPP, MOST PROBABLE SPEED ( $v_{mp}$ ), AND IVRT FOR THE ANALYZED GASES

Gas	Mass (u)	MPP (m)	$v_{mp}$ (m/s)	IVRT (s)
H <sub>2</sub>	2	821	1561.21	0.526
He	4	706	1103.94	0.638
Ne	20	569	493.70	1.151
N <sub>2</sub>	28	566	417.25	1.360
Ar	40	615	349.10	1.787

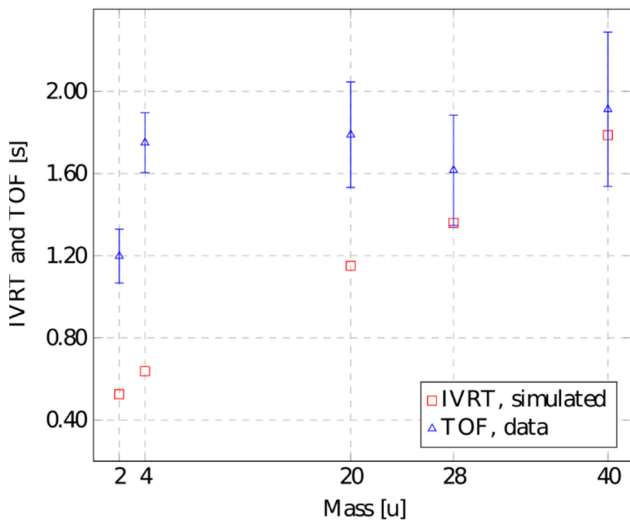


Fig. 4. Comparison of Table II values (red squares) with the P-DRGA data (blue triangles) from [4]. Error bar of experimental data is the standard deviation of the measurement. (Color online.)

the vacuum vessel. Using this feature, the program computes the average distance traveled by a large number of particles before they are pumped; this distance can be called the mean pumping path (MPP). By dividing the MPP for the most probable speed of the gas molecule

$$v_{mp} = \sqrt{\frac{2RT}{M_{mol}}}$$

The average time that the gas particles reside into the DRGA chamber can be calculated; this time can be called IVRT. During this time, the particle has a certain probability of being detected, and because the RGA is positioned very close to the TMP, the IVRT is equivalent to the TOF as it has been called in other publications. Simulations for H<sub>2</sub>, He, Ne, N<sub>2</sub>, and Ar at 293.15 K were made and the IVRT computed as previously described. For all the simulations, the injected throughput and TMP pumping speed were recalculated to consider the gas under test. The simulation results are shown in Table II and compared to experimental results in Fig. 4. From comparison, we draw the following conclusions.

- 1) The theoretical data for H<sub>2</sub> and He underestimate the experimental value. This fact can be explained by a back-streaming of these light gases through the TMP, with H<sub>2</sub> and He that returns in the RGA chamber after

being pumped. Back-streaming is a known issue [10] and can be avoided by improved fore vacuum condition of the primary TMP, e.g., by introducing another TMP in the fore vacuum line.

- 2) The experimental and theoretical data for Ne differ significantly. This can be explained by the fact that due to the lack of measured data from the vendor, the Ne pumping speed was set to the nominal speed of the TMP. Additionally, the RGA mass peak at 20  $\mu$  is not only exclusive to Ne but also prominent in the water cracking pattern, which leads to greater deviations.
- 3) The data for N<sub>2</sub> and Ar lay within the error of the measured data.

## V. OGA IMPROVEMENT

The OGA, a spectroscopic observation of a cold plasma discharge of residual gas at elevated pressure, is a secondary system for gas composition analysis included in the DRGA system [1].

The fitness of the concept to differentiate between fusion products, not only for hydrogen isotopes [11] but also for helium isotopes, has been demonstrated at Joint European Torus (JET) [12]. The original hardware for the P-DRGA OGA was a rather dated Alcatel CF2 Penning gauge, a system primarily designed as a pressure gauge and not optimized for light yield for spectroscopic observation. Also, this hardware is long out of commercial production. The experiments at JET utilize a similar, although slightly adapted device.

There exists, however, a Penning gauge optimized for spectroscopic analysis in fusion divertor conditions, and the Wisconsin *In situ* Penning (WISP) gauge developed for sub-divertor partial pressure analysis at W7-X [13]. Aimed at divertor-relevant pressures, with an experimentally observed lower limit  $1 \times 10^{-2}$  Pa in W7-X OP1.2, the current WISP setup cannot directly be used in the P-DRGA OGA, which operates at about  $1 \times 10^{-3}$  Pa. Both pressure reading and light yield become unreliable at these pressures, but the challenges are possible to overcome. Furthermore, the standard WISP is equipped with loadlock-like apparatus, which enables its placement inside the main vacuum chamber, and its performance is optimized for the strong magnetic confinement fields in which it operates. In principle, a combination of a lower magnetic field at the OGA, e.g., via a permanent magnet clamped onto the outside of the cathode, and a high anode potential can be envisaged to extend the operation regime down to lower pressures. At low magnetic fields, mode switching has been observed [13] but seems to be avoidable by proper field strength selection. Finally, the magnetic field arrangement has to be such that magnetic leakage is minimized (the OGA plasma source in the DRGA analysis station arrangement is in close proximity to the TMP) and also minimally perturbed by external magnetic fields, since magnetic shield may be impractical for the location of the OGA. Development of such a modified (*ex situ*) version of the WISP is currently under consideration. Other alternative plasma sources meeting these requirements are currently being sought, in synergy

with the ongoing ITER DRGA design project, which is the responsibility of U.S. ITER.

## VI. CONCLUSION

We have discussed the current state of improvements on the P-DRGA currently deployed at W7-X.

A new magnetic shielding for the mass spectrometers has been designed, manufactured, and tested. The results are promising and give rise to hope for future unperturbed mass spectrometer operation.

The Molflow+ simulation of the gas flow confirms the measured TOF for heavier gases and indicates a back-streaming effect for lighter gases.

Improvement of the OGA with a WISP gauge has turned out to be less straightforward than anticipated but seems possible and promising and will be pursued further.

## ACKNOWLEDGMENT

The authors would like to thank laboratory support by A. von Stechow, N. Paschkowski, and C. Ahrens and would also like to thank the CVP image by M. Weißgerber.

This work has been carried out within the framework of the EUROfusion Consortium, funded by the European Union via the Euratom Research and Training Programme (Grant Agreement No. 101052200—EUROfusion). Views and opinions expressed are however those of the author(s) only and do not necessarily reflect those of the European Union or the European Commission. Neither the European Union nor the European Commission can be held responsible for them.

## REFERENCES

- [1] C. C. Klepper *et al.*, “Design of a diagnostic residual gas analyzer for the ITER divertor,” *Fusion Eng. Des.*, vols. 96–97, pp. 803–807, Oct. 2015.
- [2] C. W. Hicks, M. E. Barber, S. D. Edkins, D. O. Brodsky, and A. P. Mackenzie, “Piezoelectric-based apparatus for strain tuning,” *Rev. Sci. Instrum.*, vol. 85, no. 6, Jun. 2014, Art. no. 065003.
- [3] T. Klinger *et al.*, “Overview of first Wendelstein 7-X high-performance operation,” *Nucl. Fusion*, vol. 59, no. 11, 2019, Art. no. 12004.
- [4] G. Schlisio *et al.*, “First results from the implementation of the ITER diagnostic residual gas analyzer prototype at wendelstein 7-X,” *Rev. Sci. Instrum.*, vol. 90, no. 9, Sep. 2019, Art. no. 093501.
- [5] V. V. Yashchuk, S. Lee, and E. Paperno, “Magnetic shielding,” in *Optical Magnetometry*, D. Budker and D. J. Kimball, Eds. Cambridge, U.K.: Cambridge Univ. Press, 2013, pp. 225–248.
- [6] C. M. Francke, *Plasma Sources Sci. Technol.*, vol. 14, pp. 226–235, 2005. [Online]. Available: <https://iopscience.iop.org/article/10.1088/0963-0252/14/2/003>
- [7] R. Kersevan and J.-L. Pons, “Introduction to MOLFLOW+: New graphical processing unit-based Monte Carlo code for simulating molecular flows and for calculating angular coefficients in the compute unified device architecture environment,” *J. Vac. Sci. Technol. A: Vac., Surf., Films*, vol. 27, no. 4, pp. 1017–1023, Jul. 2009.
- [8] R. Kersevan and M. Ady, in *Proc. 10th Int. Part. Accel. Conf.*, Melbourne, VIC, Australia, May 2019, doi: [10.18429/JACoW-IPAC2019-TUPMP037](https://doi.org/10.18429/JACoW-IPAC2019-TUPMP037).
- [9] C. C. Klepper and F. A. Ravelli, “Monte Carlo analysis of the performance of the ITER diagnostic residual gas analyzer,” *Fusion Sci. Technol.*, vol. 77, nos. 7–8, pp. 629–640, Nov. 2021.
- [10] I. Bello, *Vacuum and Ultravacuum: Physics and Technology*, 1st ed. Boca Raton, FL, USA: CRC Press, 2017.
- [11] D. L. Hillis, *Rev. Sci. Inst.*, vol. 70, no. 1, 1999, doi: [10.1063/1.1149301](https://doi.org/10.1063/1.1149301).
- [12] S. Vartanian *et al.*, “Simultaneous H/D/T and 3He/4He absolute concentration measurements with an optical Penning gauge on JET,” *Fusion Eng. Des.*, vol. 170, Sep. 2021, Art. no. 112511.
- [13] T. Kremeyer, K. Flesch, O. Schmitz, G. Schlisio, U. Wenzel, and W.-X. Team, “Wisconsin *in situ* Penning (WISP) gauge: A versatile neutral pressure gauge to measure partial pressures in strong magnetic fields,” *Rev. Sci. Instrum.*, vol. 91, no. 4, Apr. 2020, Art. no. 043504.



**Georg Schlisio** received the Ph.D. degree from Universität Greifswald, Greifswald, Germany, in 2021, after working on gas balances for Wendelstein 7-X (W7-X), where he continues his position as a postdoctoral.

His current focus of work is the operation and improvement of the prototype diagnostic residual gas analyzer (P-DRGA) and the neutral pressure gauges at W7-X and their utilization for exhaust quantification and optimization.

**Fabio A. Ravelli** received the master’s degree in physics in 1993, with a thesis on experimental plasma physics.

Since then, he has covered Research and Development positions in various industrial vacuum technology companies, developing ultra-high vacuum (UHV) pumping solutions and vacuum deposition tools for the semiconductor and touch panels market. In 2016, he joined European Spallation Source, Lund, Sweden, as a Vacuum Engineer for the superconducting particle free proton accelerator. In 2019, he joined U.S. ITER, Oak Ridge, TN, USA, and since 2020, he has been with Commonwealth Fusion System, Cambridge, MA, USA, as the Lead of the Vacuum Group delivering pumping systems for magnetically confined nuclear fusion machines. His interests in vacuum technology span a large application spectrum, from thin-film deposition tools to ultrahigh vacuum particle free systems for particle generator and to the development of vacuum pumps for the treatment of tritiated gas streams.



**C. Christopher Klepper** (Senior Member, IEEE) received the Ph.D. degree from The University of Texas at Austin, Austin, TX, USA, in 1985. His dissertation was related to recycling of hydrogen from solid surfaces into the hot fusion plasma.

He worked with the Department of Energy (DOE) Magnetic Fusion Energy (MFE) project called the Texas Experimental Tokamak at The University of Texas at Austin. From 1985 to 1997, he was a Research Staff with the Oak Ridge National Laboratory (ORNL), Oak Ridge, TN, USA, where he pursued his interest in both MFE- and materials-processing-related plasmas. From 1997 to 2009, he was a Research Scientist with HY-Tech Research Corporation, Radford, VA, USA. He was a principal investigator in several federally funded projects, most in partnerships with DOE laboratories or industry. These have led to the development of new materials processing technologies, including cathodic arc-deposited super-hard, boron-based coatings, microwave sintering to produce robust cathodes from boron and boron carbide powders, and a neutron-detector manufacturing process. In 2009, he rejoined ORNL, where he is currently working toward plasma-wall interaction studies near RF-heating components, primarily in the European large fusion energy experiments, including Tore Supra (now WEST) and JET (with ITER-Like Wall and through deuterium-tritium campaign 2). He has been leading the technical side of the U.S.-ITER project to design and build a diagnostic residual gas analyzer (DRGA) for ITER, since 2010, where he is currently a member of the ITPA Diagnostics Topical Group. He has authored or coauthored more than 150 journal articles.

Dr. Klepper is a member of APS and an alumnus of Sigma Pi Sigma and Phi Beta Kappa.



**Jeffrey H. Harris** received the B.S. and M.S. degrees from the Massachusetts Institute of Technology (MIT), Cambridge, MA, USA, and the Ph.D. degree from the University of Wisconsin–Madison, Madison, WI, USA.

He has worked on magnetic fusion experiments in the USA, Russia, Japan, France, Australia, and Germany.



**Theodore M. Biewer** received the B.S. and B.A. degrees from Arizona State University, Tempe, AZ, USA, and the M.S., M.S., and Ph.D. degrees from the University of Wisconsin–Madison, Madison, WI, USA. He is currently a Senior Scientist with the Oak Ridge National Laboratory (ORNL), Oak Ridge, TN, USA, where he is a Diagnostics and Control Group Leader with the Fusion Energy Division. To facilitate the mentoring of Ph.D. students at ORNL, he received a Joint-Faculty Associate Professorship from the Bredesen Center, The University of Tennessee at Knoxville, Knoxville, TN, USA.



**Dirk Naujoks** studied at the Moscow Institute of Energy, Moscow, Russia (1983–1989). He received the Ph.D. degree from Lomonosov Moscow State University, Moscow, in 1991, and the Habilitation degree from the Humboldt University of Berlin, Berlin, Germany.

Since 1991, he has been with the Max Planck Institute for Plasma Physics (IPP), Greifswald, Germany, at the Garching and Berlin sites, where he is currently participating in the IPP's Wendelstein 7-X (W7-X) stellarator project in Greifswald. In 1999, he spent six months as a Visiting Scientist with the Argonne National Laboratory, Lemont, IL, USA. From 2001 to 2005, he lectured on plasma physics and computer simulation with the Humboldt University of Berlin.



**Chris Marcus** received the B.S. degree in chemistry from The University of Tennessee at Knoxville, Knoxville, TN, USA, in 1986, and the M.B.A. degree from Loyola Marymount University (LMU), Los Angeles, CA, USA, in 1990.

He has performed research, in support of U.S.-ITER Diagnostics Projects, for several years as well as worked in the field of isotopic enrichment technology. Specific to fusion energy research, he has made many contributions in the selection, assembly, and development of hardware associated

with the concept for the diagnostic residual gas analyzer system. He has an extensive background in applications for both high vacuum technology and gas processing techniques.



**Amit K. Kharwandikar** is currently pursuing the Ph.D. degree with the Stellarator Edge and Divertor Physics Department, Max Planck Institute for Plasma Physics (IPP), Greifswald, Germany.

His work focuses on divertor optimization for Wendelstein 7-X (W7-X).



**Thierry Kremeyer** currently holds a post-doctoral position with the Max Planck Institute for Plasma Physics, Greifswald, Germany, where he works in understanding the hydrogen fuel cycle and exhaust with the island divertor. He takes care of a camera network that permits full divertor observation. This data allowed him to quantify the recycling flux and close a single reservoir particle balance. In the future, he would like to solve the problem of designing a reactor relevant island divertor with a target geometry that allows for efficient exhaust in a stellarator.